JOURNAL OF MATERIALS SCIENCE 30 (1995) 4407–4416

Conduction mechanism in composite solid electrolytes: PbX_2–Al_2O_3 (X = Cl, Br, I) systems

A. KUMAR, K. SHAHI
Department of Physics and Materials Science Programme, Indian Institute of Technology, Kanpur 208 016, INDIA

Composite solid electrolytes PbX_2–Al_2O_3 (X=Cl, Br, I) have been synthesized by the powder metallurgical process, and investigated by complex impedance analysis, X-ray diffraction (XRD), differential thermal analysis (DTA) and scanning electron microscope (SEM) techniques. The phase analyses reveal that the composites are two-phase systems. No chemical reaction nor solid solution formation takes place between Al_2O_3 and the respective matrix phases. SEM photomicrographs show that Al_2O_3 particles are uniformly dispersed in the matrix phase for various systems. While $PbCl_2$–Al_2O_3 and $PbBr_2$–Al_2O_3 composites show a decrease in conductivity over their respective pure phases; PbI_2–Al_2O_3 composites exhibit enhanced conductivity. By using the known diffusion and mobility data of the mobile species it has been shown that enhancement in conductivity is possible only in case of PbI_2.

1. Introduction

Dispersion of second phase fine insulating particles (dispersion hardening) is a well known method to improve the mechanical properties of materials. Its electrical analogue was discovered by Liang [1] in the LiI–Al_2O_3 system, in which he observed that ionic conductivity increased by orders of magnitude. Since then, enhancement in ionic conductivity in a number of normal ionic conductors has been reported. The systems investigated include both cationic conductors, such as alkali, silver and copper halides [2–6], and anionic conductors, such as CaF_2, BaF_2, $SrCl_2$ and HgI_2 [7–10]. In stark contrast to the general trend, Brune and Wagner [11] reported a decrease in conductivity of $PbCl_2$ containing dispersion of Al_2O_3 particles. However, the PbI_2–Al_2O_3 system investigated recently [12] exhibits enhanced conductivity and hence follows the general trend. This paper reports a comprehensive study of the three lead halides, namely PbX_2–Al_2O_3 (X = Cl, Br, I) systems, and examines if the data on these anomalous systems lead to a new insight into the conduction mechanism in composite solid electrolytes.

2. Experimental procedure

High purity $PbCl_2$ and $PbBr_2$ were obtained from Aldrich Chemicals, Inc. USA and PbI_2 was procured from Alfa products. Deagglomerated Al_2O_3 powder of three different particle sizes (0.05, 0.3 and 1.0 μm) was obtained from Buehler Micropolish II (USA). PbX_2–Al_2O_3 (X = Cl, Br, I) composites of various compositions have been prepared by two slightly different ways. In the first case, appropriate amounts of the constituents are mixed, milled and ground followed by pelletization (method I). In the second method the mixture obtained after regrinding was heated above the melting point of the respective lead salt before pelletization to ensure homogeneous dispersion of Al_2O_3 particles in the matrix phase (method II). The pressed pellets of $PbCl_2$–Al_2O_3 are sintered at 450° C, $PbBr_2$–Al_2O_3 at 350° C and PbI_2–Al_2O_3 at 320° C for ~20–24 h.

The composite samples have been investigated by XRD and DTA for phase characterization and to find out the solubility (if any) of Al_2O_3 in the matrix phase, and also by SEM to examine the distribution of Al_2O_3 particles in the matrix phase. The details of various techniques are given elsewhere [12]. The impedance measurements were carried out using an HP-4192A impedance analyser. The d.c. electrical conductivity of various samples was obtained at each temperature from the complex impedance analysis [13]. The resistance obtained from the high frequency semicircular portion of the complex spectra was used to calculate the d.c. conductivity of each sample.

3. Results and discussion

3.1. Differential thermal analysis

The DTA results for pure $PbCl_2$ and $PbCl_2$–3O mol% Al_2O_3 samples prepared by methods I and II are shown in Fig. 1. In each case only one endothermic peak corresponding to the melting of $PbCl_2$ is observed, leading to the obvious conclusion that Al_2O_3 remains as a separate phase in $PbCl_2$–Al_2O_3 composites prepared by both methods and that no chemical reaction takes place between the two components. The decreased peak heights and peak areas for $PbCl_2$–3O mol % Al_2O_3 composites (curves b and c in Fig. 1) are merely due to the lower concentration of $PbCl_2$ in the composites compared to the pure salt (curve a).

0022–2461

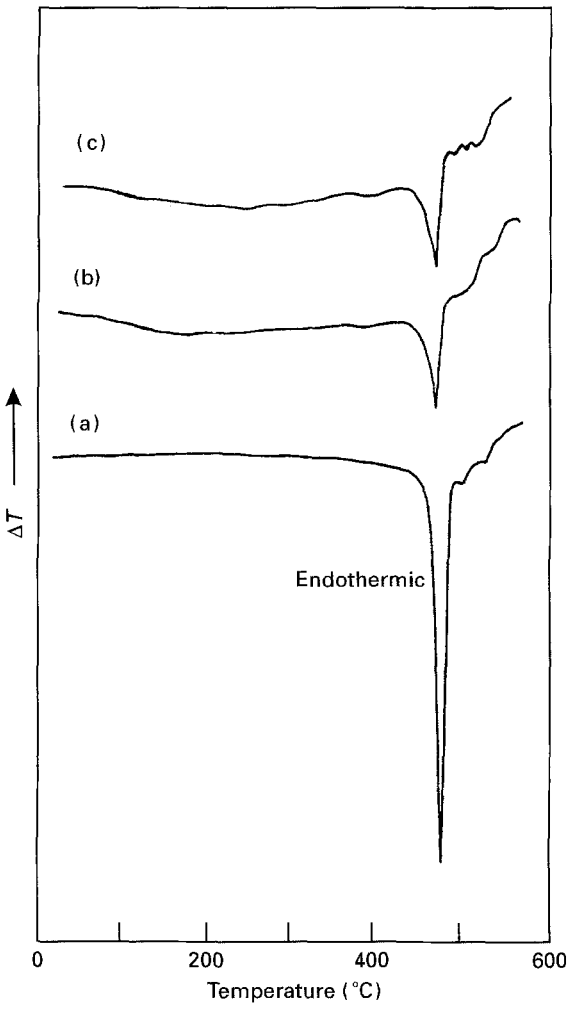

Figure 1 DTA curves for (a) $PbCl_2$, $PbCl_2$–3O mol% Al_2O_3 composite prepared by (b) method I, and (c) method II.

The DTA results on $PbBr_2$ and $PbBr_2$–Al_2O_3 composites are found to be similar, and hence lead to identical conclusions, namely no chemical reaction or solid solution formation takes place between the two constituents, $PbBr_2$ and Al_2O_3 remaining as separate phases in the composite.

Fig. 2 shows the DTA curves for pure PbI_2 and PbI_2–30 mol % Al_2O_3 composites prepared by methods I and II. The lone peak appearing in the case of PbI_2 (curve a) is due to melting of PbI_2. Curve (b) for the PbI_2–30 mol % Al_2O_3 sample prepared by method I also exhibits a peak corresponding to the melting of pure PbI_2 which implies that the PbI_2 in the composite remains as a separate phase at least up to the melting point of PbI_2. However, an additional (though minor) exothermic peak appears at $\sim 450°$ C which may be due to

1. decomposition of PbI_2,
2. release of adsorbed water molecules on the Al_2O_3 surface, or
3. some chemical reaction between the constituents.

The DTA curve of the sample prepared by method II does not show any thermal event (peak) in the investigated temperature range, which suggests that PbI_2 is no longer present in the composite, and that the sample is a chemically different material. The

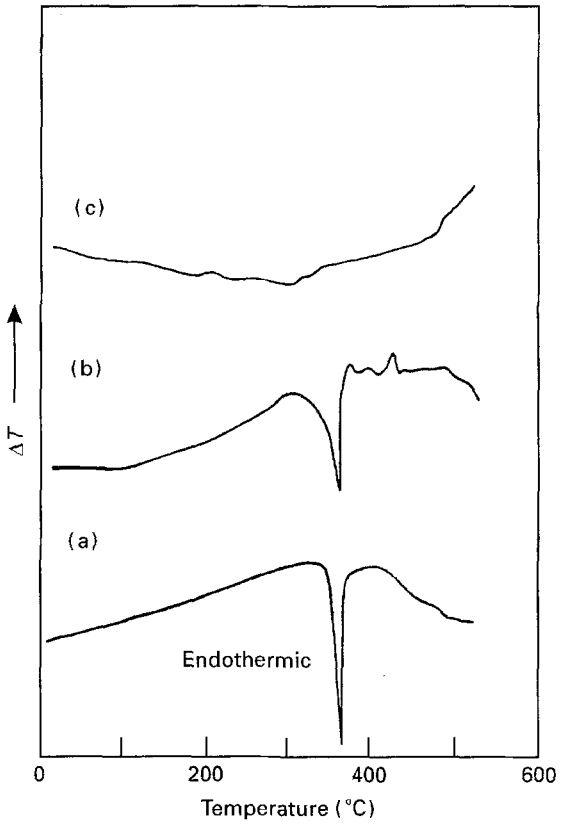

Figure 2 DTA curves for (a) PbI_2, PbI_2–3O mol% Al_2O_3 prepared by (b) method I, and (c) method II.

observed change of colour of the sample also suggests that a chemical change takes place in those samples prepared by method II. It is thus inferred that the samples prepared by method I are two-phase (PbI_2–Al_2O_3) composites, and those prepared by method II, wherein the constituents are heat treated above the melting point of PbI_2, are not two-phase composites.

3.2. X-ray diffraction

Fig. 3 shows the XRD patterns for $PbCl_2$–30 mol % Al_2O_3 composites prepared by methods I and II. These results show that heat treatment (method II; curve b) does not affect the X-ray diffraction patterns; which signifies that no chemical reaction or solid solution formation takes place between $PbCl_2$ and Al_2O_3 even after heat treatment. However, since the XRD patterns were recorded at room temperature, it is possible that some new phase or solid solution formation occurs at higher temperature, but at room temperature the two parent phases, (namely $PbCl_2$ and Al_2O_3), separate out. This possibility is, however, ruled out by the DTA studies reported above.

The XRD patterns of $PbBr_2$–30 mol % Al_2O_3 at room temperature with and without heat treatment (at 350° C) were also found to be identical and could either be attributed to $PbBr_2$ or to Al_2O_3. The combined DTA and XRD results rule out the possibility of any chemical reaction or formation of any new phase between $PbBr_2$ and Al_2O_3.

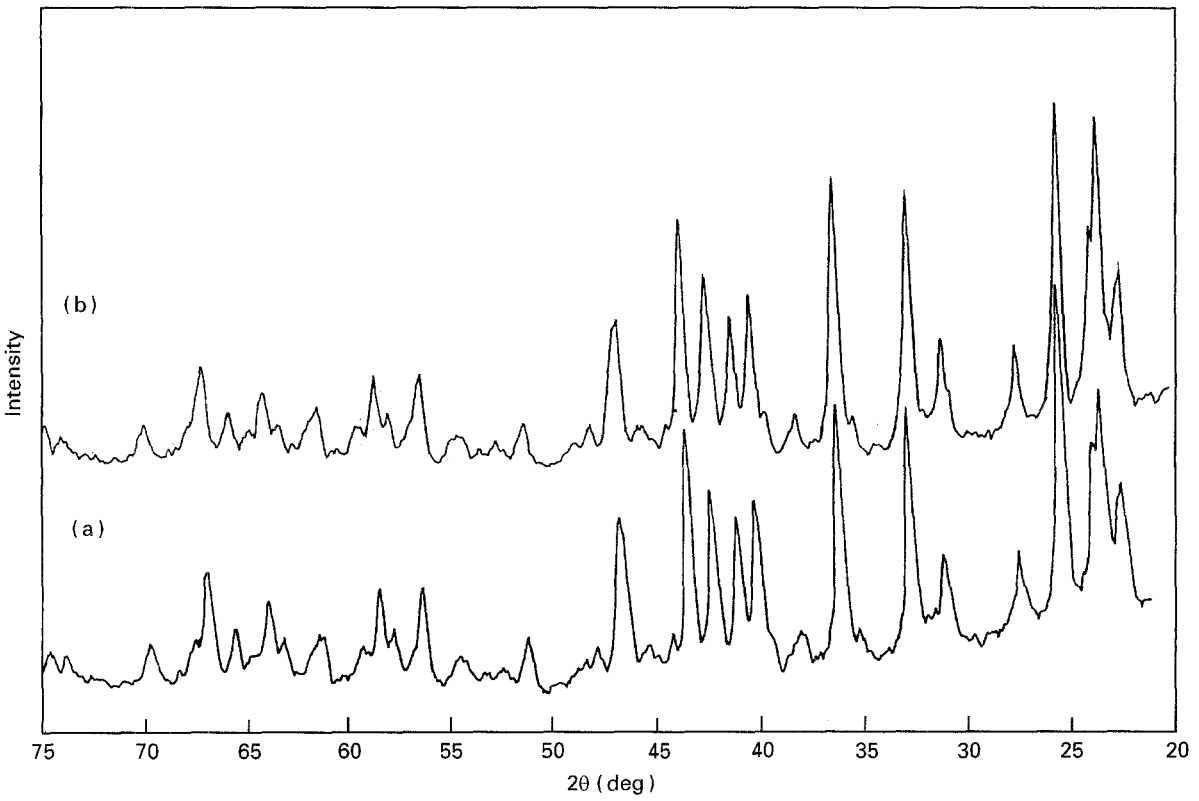

Figure 3 XRD patterns for $PbCl_2$–3O mol% Al_2O_3 samples prepared by (a) method I and (b) method II.

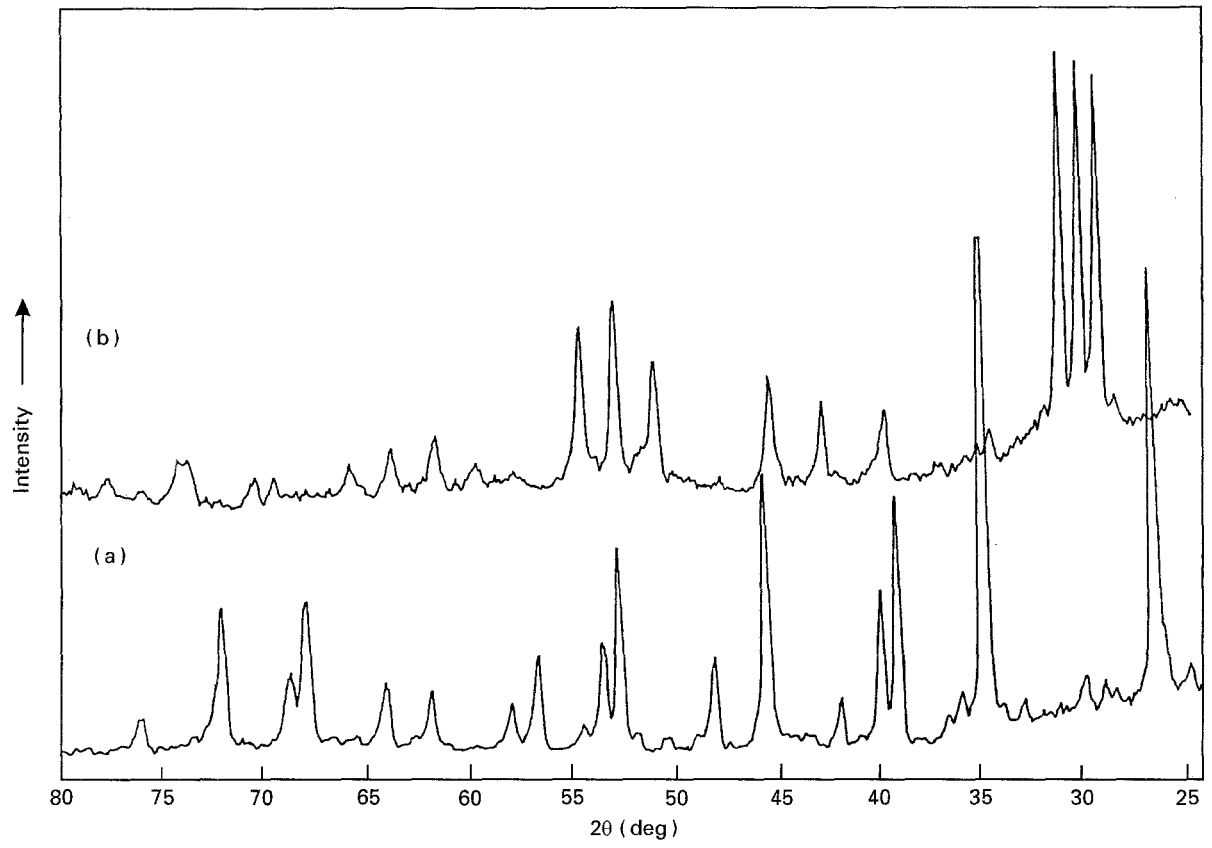

Figure 4 XRD patterns for PbI_2–3O mol% Al_2O_3 samples prepared by (a) method I and (b) method II.

Fig. 4 shows the XRD patterns at room temperature for PbI_2–30 mol % Al_2O_3 composites prepared by methods I and II. The XRD pattern for the sample prepared by method II (curve b) does not contain even the prominent peaks present in curve a. Moreover, it contains several major peaks, which are not at all present in curve a. These, together with the DTA results, clearly suggest that the sample prepared by

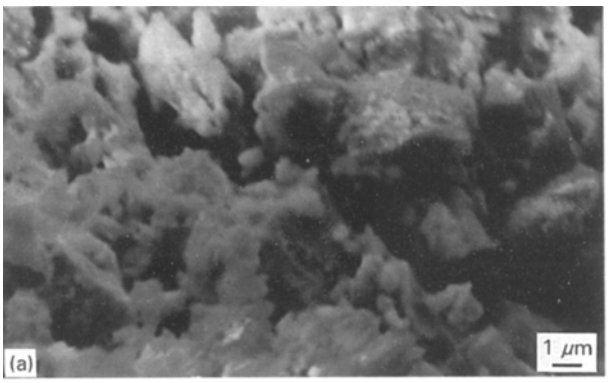

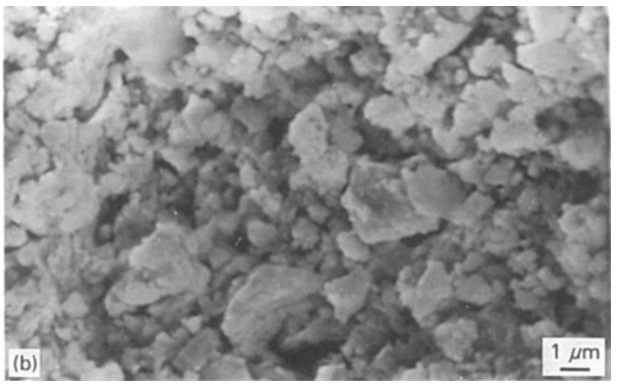

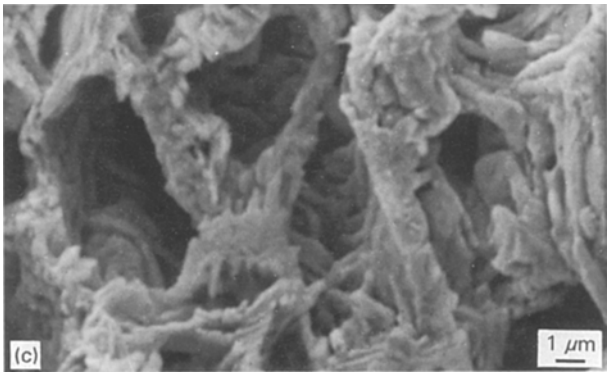

Figure 5 SEM micrographs for (a) $PbCl_2$–3O mol% Al_2O_3 composite sintered at 450° C, (b) $PbBr_2$–3O mol% Al_2O_3 composite sintered at 350° C, and (c) PbI_2–3O mol% Al_2O_3 composite sintered at 320° C.

method II is a chemically different material, and not a two-phase composite of PbI_2 and Al_2O_3.

3.3. Scanning electron microscopy

Fig. 5a is an SEM micrograph of a well polished sample of $PbCl_2$–30 mol % Al_2O_3 sintered at 450° C for ~20 h. It is observed that Al_2O_3 particles are dispersed in $PbCl_2$ grains. Thus, Al_2O_3 remains as a separate phase and the $PbCl_2$–Al_2O_3 system forms a two-phase composite.

The SEM studies for a $PbBr_2$–30 mol % Al_2O_3 sample sintered at 300° C (Fig. 5b) also suggest that the system is a composite, wherein Al_2O_3 particles are dispersed in $PbBr_2$ grains.

Fig. 5c shows the SEM micrographs of well polished samples of a PbI_2–30 mol % Al_2O_3 composite prepared by method I, sintered at 320° C, well below the melting point of PbI_2 (402° C). The microstructure shows that the Al_2O_3 particles are well dispersed in the PbI_2 matrix. Thus, the samples prepared by method I form a two-phase composite.

3.4. Conductivity versus composition

The conductivity isotherms for $PbCl_2$–Al_2O_3 composites at three different temperatures, namely 100, 200 and 300° C, are shown in Fig. 6. It is found that as the concentration of Al_2O_3 increases the conductivity decreases monotonically. This behaviour is in stark contrast to most of the reported results on composite solid electrolytes, which show substantial enhancement in conductivity instead. It appears that

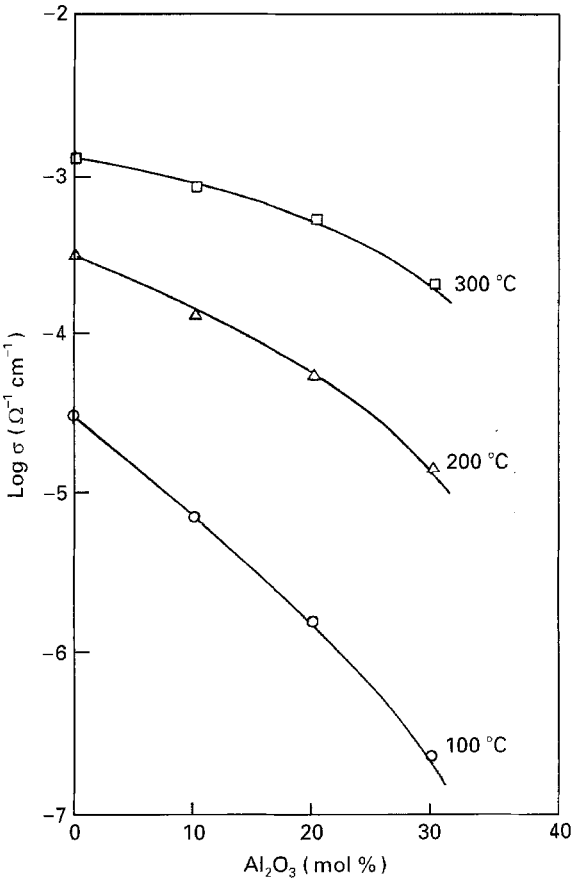

Figure 6 Log σ versus composition (mol% of Al_2O_3) for $PbCl_2$–Al_2O_3 composites at three different temperatures.

TABLE I Normalized conductivity, σ/σ_o, for $PbCl_2$–Al_2O_3 composites of various compositions at three different temperatures

Composition Al_2O_3[a]		σ/σ_o		
(mol %)	(vol %)	300 °C	200 °C	100 °C
0	0	1.00	1.00	1.00
10	6	0.63	0.41	0.22
20	12	0.40	0.17	0.05
30	19	0.16	0.05	7.20×10^{-3}

[a] The particle size of Al_2O_3 used in this work is 0.05 μm unless otherwise specified.

in $PbCl_2$–Al_2O_3 composites a high conducting layer does not form and the addition of an insulator results in dilution of conductivity. Table I compares the normalized conductivity, the ratio of the conductivity of the composite to that of pure salt, σ/σ_0, for the $PbCl_2$–Al_2O_3 composites at three different temperatures. It is observed that the decrease in conductivity is higher at lower temperatures.

$PbCl_2$ is known to be an anionic conductor [14, 15] and exhibits Schottky disorder owing to the larger size of chloride ions [16–18] and the narrow free space around interstitial sites [19]. The cation and anion vacancies, V''_{Pb} and $V^{\cdot}_{Cl}$ are formed according to the equation

$$O \Leftrightarrow V''_{Pb} + 2V^{\cdot}_{Cl} \Leftrightarrow (V_{Pb}V_{Cl})' + V^{\cdot}_{Cl} \qquad (1)$$

One may be tempted to explain the observed decrease in conductivity due to trace amounts of dissolved Al_2O_3 in the host matrix $PbCl_2$, as it is well established that the conductivity of ionic solids doped with suitable aliovalent impurities first decreases before increasing as the dopant concentration increases [20–22]. The dissolution of Al_2O_3 in PbX_2, using Kröger–Vink notation, may be described by the following relation

$$Al_2O_3 \Leftrightarrow 2Al^{\cdot}_{Pb} + V^{\cdot}_{Cl} + 3O'_{Cl} \qquad (2)$$

Thus one molecule of dissolved Al_2O_3 produces one excess chloride ion vacancy which is also the more mobile charge carrier. Hence, conductivity should have increased due to addition of Al_2O_3, instead it decreases. Alternatively, the decrease in conductivity could have occurred as a result of chemical reaction between the constituents and formation of a new compound with lower conductivity. However, both DTA and XRD results rule out the formation of any new intermediate compound.

It would be appropriate to interpret the observed effect of dispersion of Al_2O_3 in $PbCl_2$ in terms of interaction between the nucleophilic groups on the dispersoid [5] and the anion vacancies which cause a depletion in the concentration of majority charge carriers. When Al_2O_3 is added, the positively charged species (lead ions) are attracted towards the alumina surface. Brune and Wagner [11] expected the dominant transport to change via negatively charged cation vacancies, V''_{Pb}. However, the mobility ratio, μ_{Pb}/μ_{Cl}, in $PbCl_2$ at 200° C is 4.18×10^{-5} [23], i.e. the mobility of negatively charged lead ion vacancies, V''_{Pb}, is too low to allow the cation vacancies to become the dominant ionic current carriers in the composite. Thus, it would appear that in $PbCl_2$–Al_2O_3 composites Pb^{2+} ions are attracted towards the dispersoid resulting in an increased concentration of cation vacancies, V''_{Pb}, in the space charge layer which are relatively immobile. As the product of concentrations of cation and anion vacancies is fixed at a constant temperature by the Schottky constant [22], the concentration of Cl^- ion vacancies decreases resulting in decreased conductivity in the composites.

The variation of conductivity as a function of Al_2O_3 concentration (mol %) in $PbBr_2$ at 100, 150 and 200° C, is shown in Fig. 7. Table II compares the normalized conductivity, σ(composite) $/\sigma_0$(host) of $PbBr_2$–Al_2O_3 composites at the three temperatures. It is observed that conductivity decreases monotonically as the concentration of Al_2O_3 in $PbBr_2$ increases, and that the rate of decrease in conductivity is faster at lower temperatures.

Like $PbCl_2$, $PbBr_2$ is also a predominantly anionic conductor [24] and exhibits Schottky type disorder [25]. The classical doping mechanism can be ruled out as a factor responsible for the decrease in σ of $PbBr_2$–Al_2O_3 composites, on a similar basis to that for the $PbCl_2$–Al_2O_3 system.

The decrease in conductivity of $PbBr_2$ due to dispersion of Al_2O_3 can be explained, as in the case of $PbCl_2$–Al_2O_3, if one assumes that the positively charged lead ions are attracted towards the nucleophilic groups at the alumina surface and thereby cause an increased concentration of lead ion vacancies, and hence a decreased concentration of bromide ion vacancies in the space charge layer. However, the lead ion vacancies are far less mobile ($\mu_{Pb}/\mu_{Br} \simeq 10^{-6}$ at 200° C) to become the dominant ionic charge carriers in $PbBr_2$–Al_2O_3 composites. Therefore, the space charge regions around the Al_2O_3 particles do not control the electrical conductivity of $PbBr_2$–Al_2O_3 composites, and Al_2O_3 dispersion results in the dilution of conductivity in the composites.

PbI_2–Al_2O_3 composites prepared by method II show a decrease in conductivity over that of pure PbI_2, which may be attributed to chemical reaction between the constituents [12]. However, unlike $PbCl_2$–Al_2O_3 and $PbBr_2$–Al_2O_3 systems, wherein the samples prepared by both methods I and II show a lowering in conductivity over respective pure phases, PbI_2–Al_2O_3 composites (method I) exhibit enhanced conductivity due to the dispersion of Al_2O_3 [12]. The results are further analysed below.

The variation of conductivity as a function of Al_2O_3 concentration (mol %) in PbI_2 at three different temperatures, namely 100, 150 and 250° C, is shown in Fig. 8. It is observed that conductivity increases only slightly up to about 10 mol % Al_2O_3, but rises rapidly subsequently and exhibits a maximum value at ~35 mol % Al_2O_3. As the concentration of Al_2O_3 increases further, conductivity decreases rather rapidly. Table III compares the normalized conductivity, the ratio σ(composite) $/\sigma_0$(host), for PbI_2–Al_2O_3 composites at 100, 150 and 250° C. The results show that the conductivity of PbI_2 is enhanced by a factor of

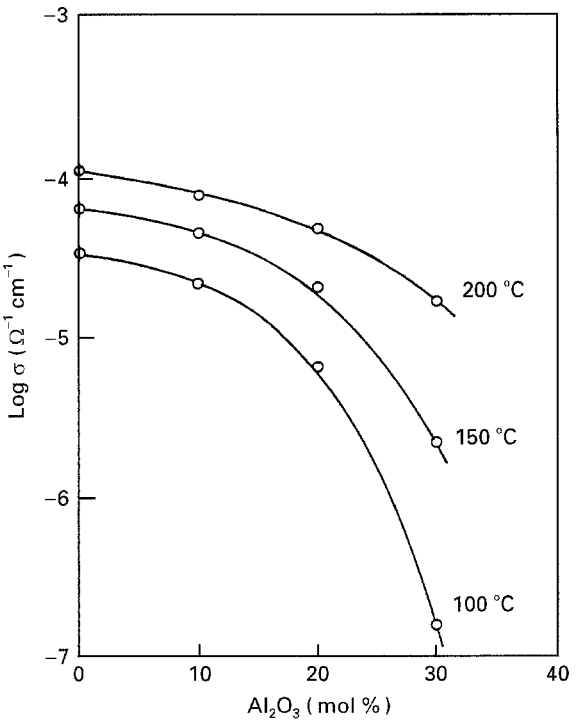

Figure 7 Conductivity versus composition (mol% of Al_2O_3) for $PbBr_2$–Al_2O_3 system at three different temperatures.

TABLE II Normalized conductivity, σ/σ_o, for various $PbBr_2$–Al_2O_3 composites at three different temperatures

Composition	Al_2O_3	σ/σ_o		
(mol %)	(vol %)	200 °C	150 °C	100 °C
0	0	1.00	1.00	1.00
10	5	0.72	0.69	0.63
20	10	0.44	0.32	0.19
30	17	0.15	3.30×10^{-2}	4.80×10^{-3}

~ 25 due to the dispersion of Al_2O_3. These results are distinctly different from those on $PbCl_2$–Al_2O_3 and $PbBr_2$–Al_2O_3 composites, which show a decrease in conductivity.

The fact that PbI_2–Al_2O_3 composites exhibit maximum conductivity at ~ 35 mol % Al_2O_3 suggests that some sort of high conducting channels form through the composite material around this composition. It could be either due to formation of a high conducting phase or a space charge layer along the interface.

PbI_2 also exhibits Schottky type disorder but, unlike in $PbCl_2$ and $PbBr_2$, both cation and anion vacancies are mobile in PbI_2 [26, 27]. A high conducting phase may form as a result of chemical reaction between PbI_2 and Al_2O_3. However, no new phase was detected by XRD at room temperature and DTA below 320 °C (samples prepared by method I). Alternatively, an enhanced conductivity phase may result due to the solubility of Al_2O_3 in PbI_2 as follows

$$Al_2O_3 \Leftrightarrow 2Al_{Pb}^{\cdot} + V_I^{\cdot} + 3O_I' \qquad (3)$$

Thus, one molecule of dissolved Al_2O_3 in PbI_2 produces one excess iodide ion vacancy, $V_I^{\cdot}$. However, if

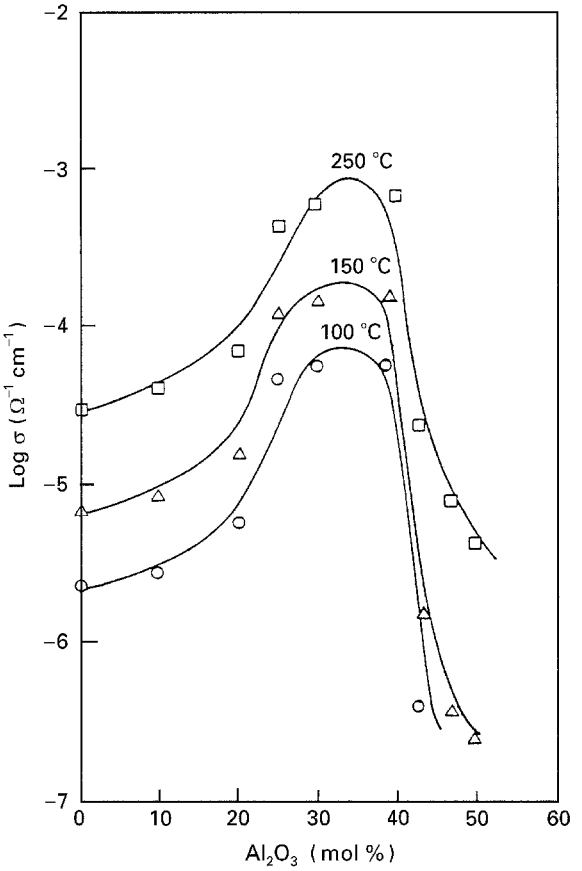

Figure 8 Conductivity versus composition (mol% of Al_2O_3) for PbI_2–Al_2O_3 composites at three different temperatures.

TABLE III Normalized conductivity, σ/σ_o, for PbI_2–Al_2O_3 composites of various compositions at three different temperatures

Composition	Al_2O_3	σ/σ_o		
(mol %)	(vol %)	100 °C	150 °C	250 °C
0	0	1.00	1.00	1.00
10	4	1.20	1.30	1.40
20	8	2.40	2.20	2.20
25	10	20.00	17.00	14.00
30	13	24.00	21.00	19.00
40	19	25.00	22.00	23.00
43	24	0.17	0.22	0.79
47	27	–	0.06	0.25
50	32	–	0.04	0.14

this were the mechanism of conductivity enhancement, only a fraction of a mole per cent of the dopant (Al_2O_3) would have been required to achieve the observed enhancement in conductivity. On the other hand, the experiments show that there is very little enhancement in conductivity due to the addition of as large as 10 mol % Al_2O_3 and that maximum enhancement in conductivity occurs at ~ 35 mol % Al_2O_3. Therefore, the classical doping mechanism does not appear to be operative in these composite solid electrolytes.

The observed enhancement in conductivity (Fig. 8) may be explained in terms of a space charge layer that may form at the interface due to interaction between the nucleophilic groups on the Al_2O_3 surface and the

positively charged species. The lead ions may be attracted towards the Al_2O_3 surface causing an increase in the concentration of cation vacancies, V''_{Pb} in the matrix in the vicinity of the interface, and simultaneously suppressing the concentration of anion vacancies, $V_I^{\cdot}$, as the product of the concentrations of cation and anion vacancies must be constant at a fixed temperature. The lead ion vacancies, V''_{Pb}, in PbI_2, unlike in $PbCl_2$ and $PbBr_2$, are relatively more mobile probably because of the high polarizability and very large size of the I^- ions (0.216 nm). Under the action of an external electric field, the I^- ions are highly polarized, thus reducing the activation barrier for Pb^{2+} ion migration. Therefore, the increased concentration and the relatively large mobility of the lead ion vacancies in the space charge region may result in enhancement of conductivity in PbI_2–Al_2O_3 composites.

3.5. Conductivity versus temperature

Fig. 9 shows the log σ versus $10^3/T$ plots for pure $PbCl_2$ and various $PbCl_2$–Al_2O_3 composites. It is observed that conductivity of the $PbCl_2$–Al_2O_3 composite decreases monotonically as the concentration of Al_2O_3 increases, and that the processing has little effect on conductivity as the results for $PbCl_2$–30 mol% Al_2O_3 composites prepared by both methods I and II are similar. Table IVa compares the ionic transport parameters, namely the overall activation energy, E_a, and the pre-exponential factor, σ_o, for pure $PbCl_2$ reported by different investigators. The E_a value found in this work agrees, within experimental error, with those reported by a majority of investigators.

The ionic transport parameters (E_a and σ_o) for various $PbCl_2$–Al_2O_3 composites are listed in Table IVb. It is noticed that the E_a value increases systematically as the concentration of the dispersed phase (Al_2O_3) increases in the composite material. It would appear that with increasing Al_2O_3 content in $PbCl_2$, the concentration of lead ion vacancies increases, which have a higher activation energy.

Fig. 10 shows the log σ versus $10^3/T$ plots for $PbBr_2$ and $PbBr_2$ containing dispersions of 10, 20 and 30 mol% Al_2O_3. These results reveal that the dispersion of Al_2O_3 results in decreased conductivity over that of pure $PbBr_2$. Table Va, b lists the Arrhenius activation energies, E_a, and the pre-exponential factors, σ_o, for $PbBr_2$ and various $PbBr_2$–Al_2O_3 composites, respectively. The E_a value for pure $PbBr_2$ obtained in this work is comparable, within experimental error, with those reported in the literature [25, 36]. As for the $PbBr_2$–Al_2O_3 composite, the E_a value keeps increasing as the concentration of Al_2O_3 in $PbBr_2$ increases, just as in the case of the $PbCl_2$–Al_2O_3 composite system.

The logarithm of d.c. conductivity, log (σ), as a function of inverse temperature for various PbI_2–Al_2O_3 composites is shown in Fig. 11. The pre-exponential factors, σ_o, and the activation energies, E_a, are given in Table VI. Unlike $PbCl_2$–Al_2O_3 and $PbBr_2$–Al_2O_3, the activation energy for conduction remains almost unchanged in PbI_2–Al_2O_3 composites, at least up to 40 mol % Al_2O_3, which would suggest that the defect and conduction mechanisms in PbI_2 do not change on addition of Al_2O_3. According to the space charge theory discussed earlier, PbI_2–Al_2O_3 composites conduct via excess Pb^{2+} ion vacancies. Thus, the fact that the migration energies in the composites and pure PbI_2 are nearly equal would suggest that Pb^{2+} ion vacancies also contribute to the conduction process in PbI_2. Unfortunately, the defect and conduction mechanisms in PbI_2 are not very well established. Nevertheless, there are a few reports [26, 27] which suggest that the migration energies and mobilities of cation and anion vacancies are comparable in PbI_2.

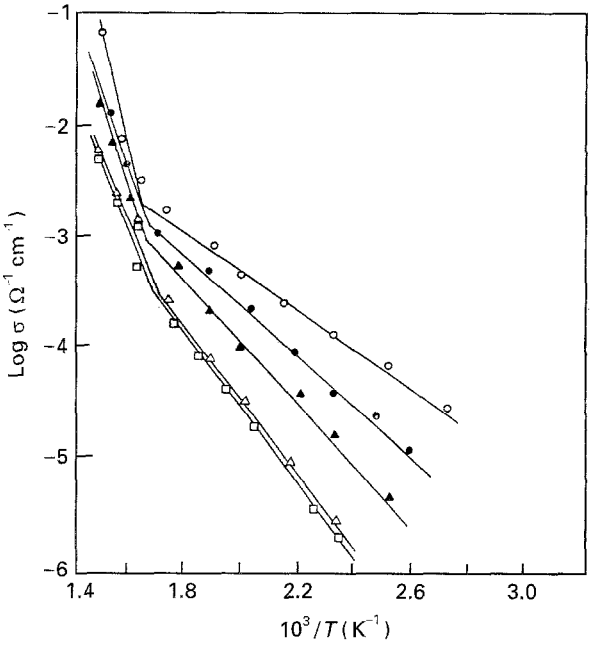

Figure 9 Log σ versus $10^3/T$ for various $PbCl_2$–Al_2O_3 composites: For (○) 0, (●) 10, (▲) 20, (△) 30, method I, and (□) 30 mol % Al_2O_3, method II.

TABLE IV Ionic transport parameters, activation energy, E_a, and pre-exponential factor, σ_o, in (a) $PbCl_2$ and (b) for various $PbCl_2$–Al_2O_3 composites in the temperature range 100–300 °C

Composition (mol %)	Al_2O_3 (vol %)	E_a (eV)	σ_o (Ω^{-1} cm^{-1})	Reference
(a) For $PbCl_2$				
		0.34	1.3	This work
		0.39	–	[28]
		0.40	8.7	[16]
		0.30	–	[17]
		0.22	–	[29]
		0.20	–	[18]
		0.35	–	[30]
		0.33	–	[31]
		0.30	–	[32]
		0.32	1.7	[33]
(b) For $PbCl_2$–Al_2O_3 composites at 100–200 °C				
0	0	0.34	1.3	
10	6	0.43	6.3	
20	12	0.54	31.0	
30 (method I)	19	0.63	70.0	
30 (method II)	19	0.64	79.0	

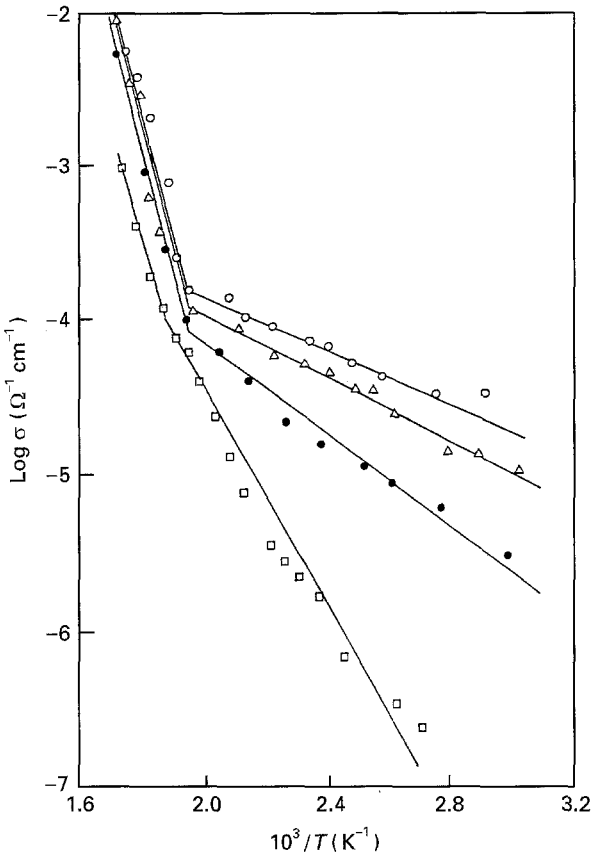

Figure 10 Log σ versus $10^3/T$ for various $PbBr_2$–Al_2O_3 composites: for (○) 0, (△) 10, (●) 20, and (□) 30 mol % Al_2O_3.

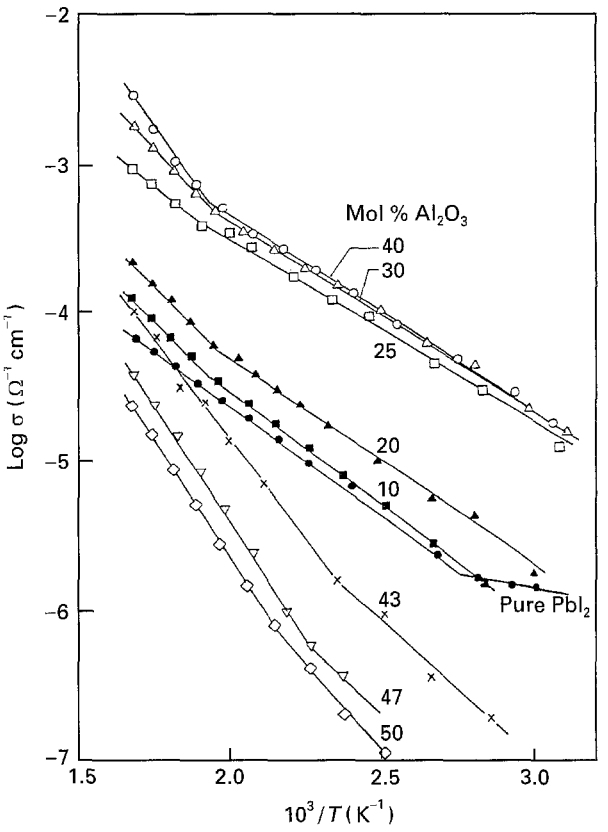

Figure 11 Log σ versus $10^3/T$ for various PbI_2–Al_2O_3 composites.

TABLE V (a) Activation energy, E_a, for conduction in $PbBr_2$ and (b) ionic transport parameters, E_a, and pre-exponential factor, σ_o, for various $PbBr_2$–Al_2O_3 composites in the temperature range 100–250 °C

Composition (mol %)	Al_2O_3 (vol %)	E_a (eV)	σ_o (Ω^{-1} cm^{-1})	Reference
(a) For $PbBr_2$				
		0.20		This work
		0.28		[34]
		0.29		[35]
		0.29		[25]
		0.25		[30]
		0.23		[36]
		0.30		[33]
(b) For $PbBr_2$–Al_2O_3 composites at 100–250 °C				
0	0	0.20	8.8×10^{-3}	
10	5	0.24	3.3×10^{-2}	
20	10	0.30	7.0×10^{-2}	
30	17	0.44	2.3×10^{-1}	

TABLE VI Ionic transport parameters, activation energy, E_a, and pre-exponential factor, σ_o, for various PbI_2–Al_2O_3 composites

Composition (mol %)	Al_2O_3 (vol %)	Temperature range (°C)	E_a (eV)	σ_o(Ω^{-1} cm^{-1})
0	0	100–300	0.29	1.9×10^{-2}
10	4	100–250	0.31	4.1×10^{-2}
20	8	100–225	0.28	3.3×10^{-2}
25	10	100–225	0.25	1.1×10^{-1}
30	13	100–225	0.26	1.7×10^{-1}
40	19	100–225	0.26	1.9×10^{-1}
43	24	100–150	0.36	3.2×10^{-2}
		175–300	0.53	3.1
47	27	125–175	0.44	6.6×10^{-2}
50	32	125–175	0.46	7.9×10^{-2}

TABLE VII Normalized conductivity, σ/σ_o, for PbI_2–30 mol% Al_2O_3 composites for three different particle sizes of Al_2O_3 at three different temperatures

Particle size of Al_2O_3, r_A (μm)	Inverse particle size, r_A^{-1} (10^4 cm^{-1})	σ/σ_o (100 °C)	(150 °C)	(250 °C)
0.05	20.0	24.0	21.0	19.0
0.30	3.3	8.9	7.8	6.5
1.00	1.0	7.1	5.9	4.5

3.6. Conductivity versus particle size

Table VII lists the particle size r_A (μm), inverse particle size, r_A^{-1} (cm^{-1}), and the normalized conductivity, σ/σ_o, at 100, 150 and 250° C for PbI_2–30 mol % Al_2O_3 composites. The fact that the relative enhancement in the conductivity is higher for lower particle sizes of Al_2O_3 suggests that the conduction mechanism must involve the matrix–particle interface.

These results are comparable to those reported earlier [2, 3, 12]. However, for a quantitative comparison between the theoretical predictions and the experiment, the electrical conductivity expression given by

Maier [5] can be rewritten as

$$\frac{\sigma}{\sigma_o} = (1 - \dot{\varphi}_A) + \frac{K}{r_A} \quad (4)$$

where

$$K = (3 \times 2^{1/2}/\sigma_o)\beta_L \varphi_A (\varepsilon\varepsilon_o RT/V^m)^{1/2} \mu_v N_{vo}^{1/2} \quad (5)$$

which is a constant at a given temperature, T, and at a fixed concentration, φ_A of the dispersoid. Other terms have their usual meaning [5]. Thus, a plot of the normalized conductivity, σ(composite) /σ_o(host), versus inverse of particle size , r_A^{-1}, should be a straight line whose slope should be equal to the constant K. Thus, the constant K can be calculated as well as determined from the experimental data, and hence compared to test Maier's theory of heterogeneous doping.

Fig. 12 shows the plot of normalized conductivity, σ/σ_o, versus inverse particle size, r_A^{-1}, at the three temperatures. Even though the graphs are reasonably good straight lines, it needs to be stressed that there are, unfortunately, only three data points corresponding to the three different particle sizes of Al_2O_3 that were available. Nevertheless, the conclusions drawn from these results may be fairly reliable, especially in view of the fact that the third data corresponding to 0.05 μm ($r_A^{-1} = 20 \times 10^4$ cm^{-1}) size of the Al_2O_3 particle is so far apart from the rest and yet falls on the line joining the other two data points (with $r_A^{-1} = 3.33 \times 10^4$ and 1×10^4 cm^{-1}). Thus, the fact that the plots are linear and their slopes decrease as temperature increases is very much in accordance with the model, which predicts that the slope K should decrease as temperature increases because at a fixed concentration φ_A of the dispersoid

$$K \propto \frac{T^{1/2}}{n_v(T)} \quad (6)$$

where $n_V(T)$ is a strong (exponential) function of temperature and thus increases much more rapidly with temperature than $T^{1/2}$, and hence K should decrease as temperature increases.

The experimental values of the slope (Fig. 12) are listed in Table VIII. In the absence of any mobility or diffusion studies on PbI_2, the conductivity of the composites and K values could not be calculated and compared with the observed values.

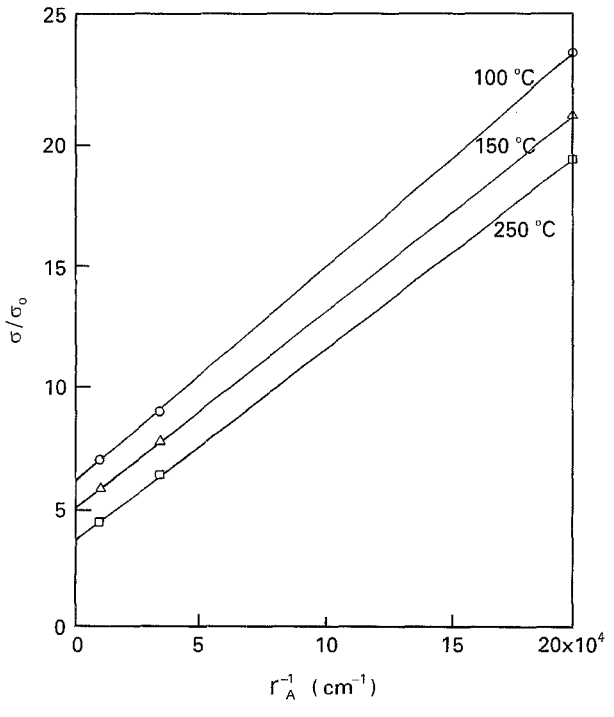

Figure 12 Normalized conductivity, σ/σ_o, versus inverse particle size, r_A^{-1}, of Al_2O_3 for PbI_2–30 mol% Al_2O_3 composites at three different temperatures.

TABLE VIII Calculated values of the slope of normalized conductivity, σ/σ_o, versus inverse particle size, r_A^{-1}, in PbI_2–30 mol% Al_2O_3 composites

Temperature (°C)	K_{cal} (cm)
300	8.7×10^{-5}
400	7.9×10^{-5}
500	7.7×10^{-5}

4. Conclusions

The compositional and particle size dependence of the conductivity of composites suggest that matrix–particle interface plays a critical role in the conductivity profiles of the composites. The PbI_2–Al_2O_3 composites show enhancement in conductivity, whereas $PbCl_2$–Al_2O_3 and $PbBr_2$–Al_2O_3 composites show a decrease in conductivity. This behaviour has been attributed to the fact that the Pb^{2+} ion vacancies are almost immobile in $PbCl_2$ and $PbBr_2$, but are as mobile as I^- ion vacancies in PbI_2. Due to Al_2O_3 dispersion the positively charged species (Pb^{2+} ions) are attracted towards the Al_2O_3 surface causing an increase in the lead ion vacancies at the interface. As the mobility of Pb^{2+} ion vacancies is comparable to that of anion vacancies, $V_I^{\cdot}$, in PbI_2, the space charge regions containing the mobile Pb^{2+} ions around the interface dominate the conduction in PbI_2–Al_2O_3 composites. This behaviour is distinctly different from the $PbCl_2$–Al_2O_3 and $PbBr_2$–Al_2O_3 composites, wherein conductivity is depressed due to decreased concentration of dominant charge carriers, chloride and bromide ion vacancies, respectively. Though the concentration of lead ion vacancies, V''_{Pb}, is increased at the interface, their mobility is negligible as compared to that of the anion vacancies. Therefore, the space charge regions at the interface do not control conduction in $PbCl_2$–Al_2O_3 and $PbBr_2$–Al_2O_3 composite systems. Thus, the results on these systems can be explained satisfactorily on the basis of space charge theory of conduction in composites solid electrolytes.

References

1. C.C. LIANG, *J. Electrochem. Soc.* **120** (1973) 1289.

2. T. JOW and J.B. WAGNER Jr, *ibid.* **126** (1979) 1963.
3. K. SHAHI and J.B. WAGNER Jr, *ibid.* **128** (1981) 6.
5. J. MAIER, *J. Phys. Chem. Solids* **46** (1985) 309.
6. *Idem, Ber. Bunsenges. Phys. Chem.* **89** (1986) 355.
7. *Idem, J. Electrochem. Soc.* **134** (1987) 1524.
8. S. FUJITSU, M. MIYAYAMA, K. KOUMOTA, H. YANAGIDA and T. KANAZAWA, *J. Mater. Sci.* **20** (1985) 2103.
9. S. FIJITSU, K. KOUMOTO and H. YANAGIDA, *Solid State Ionics* **18/19** (1986) 1146.
10. N. VAIDEHI, R. AKILA, A. K. SHUKLA and K. T. JACOB, *Mater. Res. Bull.* **21** (1986) 909.
11. A. BRUNE and J. B. WAGNER Jr, *Solid State Ionics* **25** (1987) 165.
12. A. KUMAR and K. SHAHI, *J. Mater. Sci.* **28** (1993) 1257.
13. S. BHATNAGAR, S. GUPTA and K. SHAHI, *Solid State Ionics* **31** (1988) 107.
14. C. TUBANDT, *Z. Anorg. Allgem. Chem.* **115** (1921) 105.
15. *Idem, ibid.* **29** (1923) 313.
16. G. SIMKOVICH, *J. Phys. Chem. Solids* **24** (1963) 213.
17. K. J. DEVRIES and J. H. VAN SANTEN, *Physica* **29** (1963) 482.
18. H. HOSHONO, M. YAMAZZAKI, Y. NAKAMURA and M. SHIMOJI, *J. Phys. Soc. Japan* **26** (1969) 1422.
19. H. BRAEKKEN, *Z. Krist.* **83** (1932) 222.
20. J. TELTOW, *Z. Phys. Chem.* **195** (1950) 213.
21. A. B. LIDIARD, in "Handbuch der Physik", Vol. 20, edited by S. Flugge (Springer-Verlag, Berlin, 1957) p. 216.
22. R. J. FRIAUF, in "Physics of Electrolytes", Vol. 1, edited by J. Hladik (Academic Press, London, 1972) p. 153.
23. G. M. SCHWAB and G. EULITZ, *Z. Physik Chem. (Frankfurt)* **55** (1967) 179.
24. C. TUBANDT and S. EGGERT, *Z. Anorg. Chem.* **110** (1920) 196.
25. J. SCHOONMAN and J. F. VERWEY, *Physica* **39** (1968) 244.
26. C. TUBANDT, "Handbuch der Experimentalphysik", Vol. 12 (Akademische Verlagsgesellschaft M. B. H., Leipzig, 1932) p. 383.
27. A. P. LINGRAS and G. SIMKOVICH, *J. Phys. Chem. Solids* **39** (1978) 1225.
28. Z. GYULAI, *Z. Phys.* **67** (1931) 812.
29. S. TOSHIMA, N. KIMURA, Y. NIIZEKI and T. NIKAIDO, *Denki kagaku* **36** (1968) 69.
30. W. E. VAN DEM BROM, J. SCHOONMAN and J. H. W. DE WIT, *J. Solid State Chem.* **4** (1986) 909.
31. A. K. PANSARE and A. V. PATANKER, *Pramana* **2** (1974) 282.
32. F. E. A. MELO, K. W. GARRETT, J. MENDOS FILHO and J. E. MOREIRA, *Solid State Commun.* **31** (1979) 29.
33. J. OBERSCHMIDT and D. LAZARUS, *Phys. Rev. B* **21** (1980) 5813.
34. A. SMAKULA, M. I. T. Technical Report No. **6** (Massachusetts Institute of Technology 1965).
35. J. F. VERWEY and J. SCHOONMAN, *Physica* **35** (1967) 386.
36. H. HOSHINO, S. YOKOSE and M. SHIMOJI, *J. Solid State Chem.* **7** (1973) 1.

Received 10 June 1994
and accepted 9 January 1995